KAPPA FORNACI, A TRIPLE RADIO STAR*

Andrei Tokovinin

Cerro Tololo Inter-American Observatory, Casilla 603, La Serena, Chile; atokovinin@ctio.noao.edu
Received 2012 November 24; accepted 2013 January 6; published 2013 February 12

ABSTRACT

Bright and nearby (22 pc) solar-type dwarf κ For (HIP 11072) is a triple system. The close pair of M-type dwarfs Ba,Bb with a tentative period of 3.7 days moves around the main component A on a 26 yr orbit. The mass of the "dark companion" Ba+Bb is comparable to the mass of A, causing large motion of the photo-center. The combined spectro-interferometric orbit of AB is derived, and the relative photometry of the components A and B is given. A weak signature of Ba and Bb is detected in the high-resolution spectra by cross-correlation and by variable emission in the Balmer hydrogen lines. The activity of the M dwarfs, manifested by a previously detected radio flare, is likely maintained by synchronization with their tight orbit. We discuss the frequency of similar hidden triple systems, methods of their detection, and the implications for multiple-star statistics.

Key words: binaries: general – stars: individual (HD 14802)

1. INTRODUCTION

In 1993 January, Guedel et al. (1995) detected microwave radiation from the nearby solar-type dwarf κ For. Its source was located $0\rlap{.}''23$ south of the star. At that time it was already known that κ For is a spectroscopic binary. Therefore, the authors suggested that the radio emission comes from the secondary companion, presumably a low-mass flaring dwarf. As we show below, the secondary is in fact a tight pair of M dwarfs. Despite the old age of this triple system (4–6 Gyr), fast axial rotation of the M dwarfs (hence high activity) is maintained by synchronization with the orbit.

Kappa Fornaci (HIP 11072, HD 14802, HR 895, GJ 97, $\alpha_{2000} = 2\!:\!22\!:\!32.54$, $\delta_{2000} = -23\!:\!48\!:\!58.8$) is located at a distance of 22 pc from the Sun according to the original *Hipparcos* catalog (ESA 1997) and its new reduction (van Leeuwen 2007). The *Hipparcos* satellite detected a large acceleration of 19.4 mas yr^{-2} presumably caused by the invisible (astrometric) companion (Makarov & Kaplan 2005). Gontcharov et al. (2000) collected historical astrometric data spanning half a century and suggested that the orbital period is around 26.5 yr. Later, Goncharov & Kiyaeva (2002) published the elements of the astrometric orbit with this period and with a relatively large semimajor axis of $\alpha = 0\rlap{.}''26$, noting that the "dark companion" is massive.

Radial velocity (RV) of κ For was monitored both at Lick and at La Silla in search of planetary companions. None has been found so far, but the RV trend caused by the stellar companion was obvious. Nidever et al. (2002) noted the trend, while Endl et al. (2002) published a preliminary spectroscopic orbit with a 21 yr period. Abt & Willmarth (2006) added their own observations and revised the orbit slightly, although the full orbital cycle was not yet covered. Neither of these publications mentions the astrometric results.

The astrometric and spectroscopic companion was first resolved by Lafrenière et al. (2007) in 2005 and, independently, by Tokovinin & Cantarutti (2008) in 2007. For this reason it received two confusing "discoverer" codes LAF 27 and

TOK 40 in the Washington Double Star Catalog (Mason et al. 2001).[1] By using all resolved measures and fixing the orbital period and eccentricity to those of the Gontcharov's orbit, Hartkopf et al. (2012) computed the first visual orbit of grade 4. Here we add new observations and derive the combined interferometric/spectroscopic orbit which agrees with the astrometric orbit.

SIMBAD lists 187 references to date and provides basic data on the primary companion, such as spectral type G1V, magnitudes $V = 5.19$, $B - V = 0.60$, $K_s = 3.741$, and near-solar metallicity (see the full compilation of stellar parameter measurements in Soubiran et al. 2010). The star is located above the main sequence in the $(V, B - V)$ color–magnitude diagram (CMD), being obviously evolved. Nordström et al. (2004) estimate the age of 6 Gyr by isochrone fitting. Nielsen & Close (2010) cite indirect age estimates of 4 Gyr and 6.3 Gyr from the lithium line strength and rotation, respectively. The star was observed by *Spitzer* and found to have no debris disk (Trilling et al. 2008). Yet, Nakajima & Morino (2012) claimed recently that κ For is young and belongs to the IC 2391 moving group. In calculating the kinematic parameters they overlooked the companion and used the *Hipparcos* proper motion (PM), biased by the orbit. We calculate the heliocentric Galactic velocity components of κ For from the center-of-mass PM (Gontcharov et al. 2000) and the new γ-velocity to be $[U, V, W] = [-19.5, -16.2, -9.6]$ km s^{-1} (U is positive toward the Galactic center).

In Section 2, we derive the updated orbit of the outer system AB. Then in Section 3 we evaluate the parameters of the companions and show that the secondary B is overmassive, being itself a close binary. This hypothesis is confirmed in Section 4 by direct spectroscopic detection of Ba and Bb. In the last Section 5 we discuss the implications of this finding for multiplicity statistics and exo-planet searches.

2. THE ORBIT OF AB

So far, spectroscopic, astrometric, and visual orbits of κ For were determined almost independently of each other. We add

---

* Based on observations obtained with CHIRON spectrometer at the 1.5 m CTIO telescope operated by SMARTS (NOAO program 2012B-0075), at the SOAR telescope, and at the Gemini Observatory (program GS-2012B-Q-71, PI: M. Hartung).

[1] The WDS keeps outdated tradition of assigning discoverer codes even when the duplicity was actually discovered before the first position measurement, as in the case of κ For.
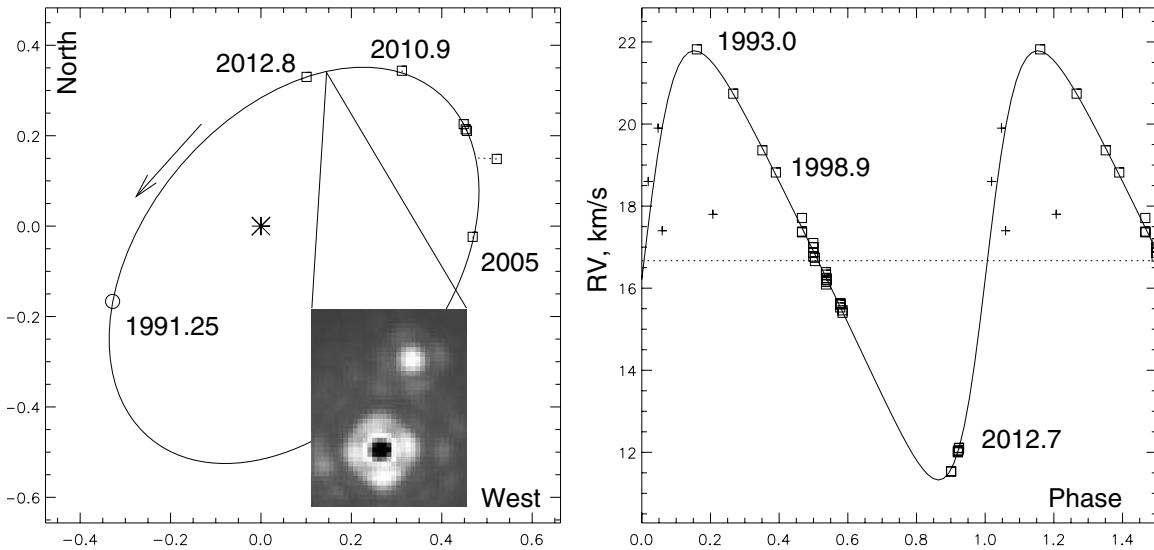
Figure 1. Combined orbit of κ For AB. Left panel: orbit in the plane of the sky, scale in arcseconds. The inset shows the *K*-band image taken at Gemini-S on 2012.67. Right panel: the RV curve with early measures plotted as crosses.

Table 1
Orbits of κ For AB

P (yr)	T (BY)	e	a (″)	Ω_A (°)	ω_A (°)	i (°)	K_1 (km s^{-1})	γ (km s^{-1})	Ref.
26.5 ± 2	1983.6 ± 2.3	0.2 ± 0.1	0.26 ± 0.01	133 ± 6	202 ± 31	56 ± 4	⋯	⋯	a
21.46 ± 0.09	1967.26 ± 1.9	0.30 ± 0.04	⋯	⋯	263 ± 12	⋯	3.95 ± 0.26	18.13 ± 0.66	b
26.5 *	2015.69	0.20 *	0.493	131.6	275.5	44.8	⋯	⋯	c
25.81 ± 0.15	1988.89 ± 0.17	0.339 ± 0.013	0.521 ± 0.004	139.8 ± 1.4	266.3 ± 1.0	50.4 ± 0.5	5.23 ± 0.13	16.67 ± 0.06	d

References. (a) Astrometric (Goncharov & Kiyaeva 2002); (b) spectroscopic (Abt & Willmarth 2006); (c) visual (Hartkopf et al. 2012); (d) combined, this work.

fresh measures and combine available data in the single orbital solution presented in Figure 1. The orbital elements and their formal errors are obtained by the unconstrained least-squares fit with weights inversely proportional to the measurement errors. The elements are listed in Table 1 together with the previously published orbits. We have not used the astrometric data of Goncharov & Kiyaeva (2002), so the good match between spectro-interferometric and astrometric orbits speaks to their veracity. This is not the case of spectroscopic orbits which have too a short period. Abt & Willmarth (2006) mention that they used "some older measures" in the orbit derivation but do not specify their source. In the future, with better RV and positional coverage, the elements will be determined to a much higher precision than here, but they will no longer be revised beyond the stated errors. The new orbit and the *Hipparcos* parallax of 45.53 ± 0.82 mas (van Leeuwen 2007) correspond to the semimajor axis of 11.44 AU and to the mass sum of 2.25 ± 0.13 $M_\odot$ (the uncertainty comes mostly from the parallax error).

RVs used in the orbit calculation are listed in Table 2. Endl et al. (2002) did not publish the RVs; three points from their Figure 6 (1993–1998) are nevertheless included in the present solution by assuming that the zero velocity in their plot corresponds to 20.36 km s^{-1}. In this case their data match well the single measurement in 1999 published by Nidever et al. (2002) and the velocities from Abt & Willmarth (2006), of which we list here only the first and the last points. The latest RV measures are obtained by the author in 2012 (see Section 4). We also use the RV measures made in Santiago in 1911–1916 with the two-prism spectrometer (Campbell & Moore 1928). Although the precision of these early data (crosses in Figure 1, right) is low, they help in constraining the orbital period.

Table 2
Radial Velocities and Residuals of κ For A

JD +2400000	RV (km s^{-1})	σ (km s^{-1})	O−C (km s^{-1})	Ref.
19378.67	18.6	2.0	1.08	a
19649.90	19.9	2.0	0.58	a
19762.62	17.4	2.0	−2.52	a
21152.78	17.8	10.0	−3.69	a
49000.0	21.82	0.2	0.04	b
50000.0	20.74	0.2	0.00	b
50800.0	19.36	0.2	−0.05	b
51170.080	18.824	0.1	0.06	c
51884.735	17.71	0.1	0.23	d
⋯	⋯	⋯	⋯	d
53001.665	15.46	0.1	0.04	d
55979.533	11.53	0.5	−0.055	e
55983.528	11.54	0.5	−0.052	e
56165.830	12.001	0.01	−0.005	e
56167.865	12.019	0.01	0.007	e
56171.797	12.032	0.01	0.008	e
56182.861	12.048	0.01	−0.009	e
56194.830	12.095	0.01	0.002	e
56200.834	12.111	0.01	−0.001	e

References. (a) Campbell & Moore 1928; (b) Endl et al. 2002, zero-point 20.36 km s^{-1}; (c) Nidever et al. 2002; (d) Abt & Willmarth 2006; (e) this work.

Positional measures of κ For AB and their residuals to the new orbit are listed in Table 3. The first measure is performed with adaptive optics, the remaining data come from speckle interferometry at the SOAR telescope in Chile. The latest speckle measure was taken at SOAR on 2012 October 29.

Table 3
Positional Measures and Residuals of κ For AB

t	θ	ρ	σ	$(O-C)_\theta, \rho$		Ref.
(yr)	(°)	(mas)	(mas)	(°)	(mas)	
2005.6348	267.1	469	5	0.4	−2	a
2007.8130	285.9	542	100	−1.7	44	b
2008.6282	294.8	502	2	−0.2	0	c
2008.6936	295.3	501	2	−0.3	−1	c
2008.8549	296.7	502	2	−0.4	0	c
2010.9655	317.8	464	2	0.6	3	d
2012.8300	343.0	345	2	0.1	0	e

References. (a) Lafrenière et al. 2007; (b) Tokovinin & Cantarutti 2008; (c) Tokovinin et al. 2010; (d) Hartkopf et al. 2012; (e) this work.

Table 4
Photometry of the Resolved Components

Parameter	V	I	H	K_s
	(mag)	(mag)	(mag)	(mag)
m_{A+B}	5.19	4.51	3.712	3.741
$m_B - m_A$	5.02 ± 0.04	3.69 ± 0.05	(2.46)	(2.14)
m_B	(10.21)	(8.23)	6.3 ± 0.2	6.0 ± 0.2

The first speckle resolution is given a low weight, considering uncertain calibration in that early experimental work.

3. PROPERTIES OF THE COMPONENTS

The component A ($V = 5.19$ mag, $B - V = 0.60$) is located $\sim1.5^m$ above the main sequence in the (M_V, $B - V$) CMD, as noted by Nordström et al. (2004). By fitting isochrones, these authors estimated the mass of the main star M_A to be between 1.12 and 1.18 $M_\odot$. We checked this against the isochrones of Girardi et al. (2000) and found that the mass of A can be as high as 1.25 $M_\odot$ if its age is 4 Gyr (it is just leaving the main sequence). It is safe to assume that $M_A = 1.20 \pm 0.05 \, M_\odot$.

The photometric data are collected in Table 4. The magnitude difference in the Strömgren y and Cousins I filters was determined by speckle interferometry at SOAR (6 and 5 independent measures, respectively); we list here the average values and their formal errors and assume $\Delta V \approx \Delta y$. The derived quantities are listed in brackets.

The flux ratio in the 1.54–1.65 μm band (which is close to H) was estimated by Lafrenière et al. (2007) as $\Delta H = 2.7 \pm 0.2$ mag. On 2012 September 2 (2012.6706), the binary was resolved with the NICI adaptive optics instrument (Chun et al. 2008); see Figure 1. As the primary companion was heavily saturated, the position measurement (340°.5, 0″.342) is not very accurate (it is not included in Table 3), and no relative photometry could be made. However, the flux from the well-resolved companion B (after halo subtraction) was estimated by comparing it to stars HIP 8674 and HIP 12425 observed before and after this target at nearly the same airmass. The H and K_s magnitudes of those two stars from Two Micron All Sky Survey (2MASS) were used to determine the zero point (the actual wavelength of the narrow-band filters was 1.587 μm and 2.272 μm). In this way we obtained crude estimates of the companion's infrared magnitudes $H = 6.0 \pm 0.2$ mag and $K_s = 6.3 \pm 0.2$ mag.

The magnitudes and colors of the companion B are thus established reasonably well, $(V - I)_B = 1.98 \pm 0.06$ and $(V - K_s)_B = 4.2 \pm 0.2$. Standard relations match those colors for a dwarf star of $\sim0.48 \, M_\odot$, but the component B is located

Table 5
Hipparcos Astrometry and the Orbit

Parameter	*Hipparcos*		Orbit ($\phi = 0.43$)	
	R.A.	Decl.	R.A.	Decl.
$\Delta\mu$ (mas yr^{-1})	1	+55	−9	+56
$\dot{\mu}$ (mas yr^{-2})	+13.0 ± 2.0	−14.4 ± 1.8	+17.7	−9.2

about 1.5^m above the main sequence in the (M_V, $V - I$) and (M_V, $V - K$) CMDs; its luminosity corresponds to a single dwarf of $\sim0.65 \, M_\odot$. This discrepancy is caused by the binary nature of B.

Large total mass of the companion B follows from the orbital parameters. Motion of the photo-center is characterized by the semimajor axis α of the astrometric orbit. Its ratio to the semimajor axis a of the visual orbit is related to the mass ratio $q = M_B/M_A$ and to the light ratio r as

$$\phi = \frac{\alpha}{a} = \frac{q - r}{(q + 1)(r + 1)}. \tag{1}$$

In our case we can neglect the companion's light because $r \approx 0.01$. The orbit of AB derived here and the astrometric orbit of Goncharov & Kiyaeva (2002) correspond to $\phi = 0.50$ and $q = \phi/(1 - \phi) = 1.0$. The companion B is therefore as massive as A while being ~100 times fainter at optical wavelengths. This finding agrees with the large orbital mass sum.

Another argument for the high companion's mass is furnished by RVs. Using the formula $a_1 \sin i = 0.01375 K_1 P (1 - e^2)^{0.5}$ (a in 10^6 km, K_1 in km s^{-1}, P in days), we obtain $a_1 = 5.53$ AU and $\phi = a_1/a = 0.48$, leading to $q = 0.93$.

The *Hipparcos* astrometry agrees very well with the new orbit if we adopt the companion's masses inferred from the photometry, $M_A = 1.20 \, M_\odot$ and $M_B = 0.96 \, M_\odot$, or $q = 0.80$ and $\phi = 0.43$. Using this ϕ, we compute the photo-center motion during the *Hipparcos* mission (mean epoch 1991.25, duration 3.2 yr). Table 5 shows that the orbital PM of the photo-center $\Delta\mu$ and its acceleration $\dot{\mu}$ match the ephemeris in both magnitude and direction. In 1991.25 the companion moved mostly to the south (see the circle in Figure 1, left), the photo-center moved to the north. The measured $\Delta\mu$ is the difference between the *Hipparcos* PM of $(+197, -5)$ mas yr^{-1} and the long-term PM of $(+196, -60)$ mas yr^{-1} derived by Gontcharov et al. (2000) from the combination of all ground-based data. The *Hipparcos* astrometry thus confirms the orbit and the fact that B is massive.

4. SPECTROSCOPY

4.1. Observations

Knowing that the companion B must be a close binary, we tried to detect this sub-system spectroscopically, despite its small contribution to the combined light. Optical spectra with resolution $\lambda/\Delta\lambda = 80,000$ were recorded with the fiber-fed CHIRON echelle spectrometer installed at the 1.5 m telescope at CTIO (Schwab et al. 2012) and operated in service mode. The object was observed in 2012 six times, on August 25, 27, 31 and September 11, 23, 29 (hereafter nights 1–6). On each visit, two 300 s exposures with the image slicer were taken, accompanied by the comparison spectrum of the thorium–argon (Th–Ar) lamp. During this period, the position of the Th–Ar spectrum remained stable on the CCD to better than 1 pixel. Moreover, on the first night the star HIP 14086 was observed as an RV reference.
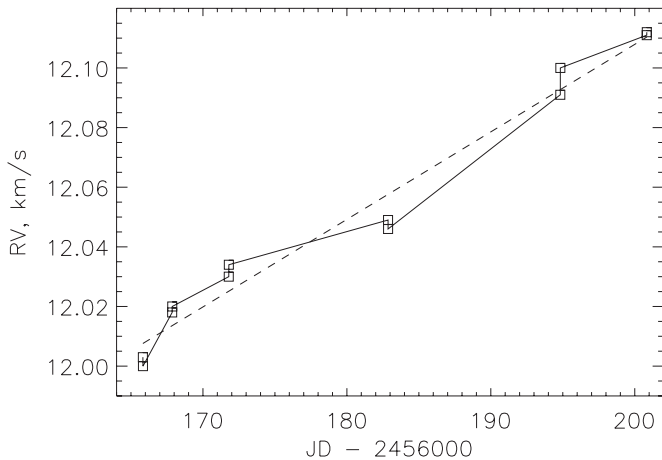
Figure 2. Radial velocity of the component A vs. time. The dashed line shows a linear fit with a slope of 2.9 m s^{-1} per day.

Extracted and wavelength-calibrated spectra were delivered by the pipeline running at Yale University. They contain 59 echelle orders (central wavelength 4605 Å–8713 Å) of 3200 pixel each (1.0768 km s^{-1} pixel^{-1}). As red orders with $\lambda > 7000$ Å suffer from extraction and calibration problems (too few thorium lines), they are not used here. The maximum intensity in the spectra varies from night to night with a total range of two times (from 25,000 to 50,000 electrons per pixel). This corresponds to a signal-to-noise ratio from 160 to 220.

4.2. Radial Velocities

RVs of κ For were derived by cross-correlating the spectra with a binary mask which equals one in the lines of the solar spectrum and zero otherwise. The mask was constructed from the digital solar spectrum (Hinkle et al. 2000),[2] binary-clipped at 0.6 of the continuum level. The cross-correlation is computed in the wavelength range from 4600 Å to 6500 Å, thus avoiding the contamination by telluric lines at longer wavelengths. Regions within ±0.5 Å of the hydrogen Balmer lines are excluded from the mask. The minimum in the cross-correlation function (CCF) is approximated by a Gaussian curve; its center is taken to be the apparent stellar RV, which is then corrected to the barycenter of the solar system in the standard way. This procedure relies on the wavelength calibration of the reduced spectra. We attempted to refine the velocity zero point by cross-correlating red orders with the mask of telluric lines, but did not obtain any trustworthy results, probably because of the poor wavelength calibration in the red.

Figure 2 shows the RVs derived from 12 individual spectra as a function of time (the average RV for each night is listed in Table 2). The linear trend of 2.9 m s^{-1} per day is caused by the orbital motion. The rms scatter of RV around this line is 6.8 m s^{-1}, and the rms residual to the orbit is 6.7 m s^{-1}. As measures from the two nightly spectra agree well, most of the scatter can be attributed to the wavelength calibration based on the Th–Ar lamp. The mean FWHM of the Gaussian fits to the CCF is 12.96 km s^{-1}, and their equivalent width is 5.59 km s^{-1}.

The same procedure applied to HIP 14086 gives an RV of +39.14 km s^{-1}. According to Nidever et al. (2002), the RV of this star is constant at +42.718 km s^{-1}, but Nordström et al. (2004) list a quite different value of +38.0 km s^{-1} (while SIMBAD lists the wrong RV of −38.4 km s^{-1}). Apparently, this star is

a yet unrecognized slow spectroscopic binary, unsuitable as an RV standard. However, we use our RV measure of HIP 14086 to derive the RV of κ For from the two spectra taken in 2012 February during CHIRON tests (those spectra lack wavelength calibration). These two measures with a somewhat uncertain zero point are given low weight in the orbit solution by adopting errors of 0.5 km s^{-1}.

4.3. Variability of the Hydrogen Line Profile

We detect a tiny variability of the Hα profile presumably caused by the moving emission of Ba and Bb. This is achieved by subtracting the template obtained by averaging all spectra together. Although the spectrometer was very stable during these observations, the spectrum moved on the CCD by 12 km s^{-1} owing to the variable barycentric correction. The template was constructed by shifting the nightly averaged spectra (with a 3 pixel median smoothing of each spectrum to remove the cosmic-ray spikes) to match the night 1, normalizing them in intensity, and adding together. Obviously, the telluric lines do not move together with the stellar lines and therefore show up in the residuals between the individual spectra and the template. The rms residuals after template subtraction are 0.7% in order 37 containing Hα and 0.5% in the blue orders which are free from the telluric lines.

We see a clear residual signal in the Hα line on the nights 1 and 5, while on the remaining nights the residuals are close to zero (Figure 3). Similar features of lower amplitude are also seen in the Hβ line, confirming their reality. The single "emission" peak on night 5 can be approximated by Gaussian curves. Their amplitude is 2.1% and 1.3% for Hα and Hβ, respectively, and they are shifted relative to the stellar spectrum by +0.28 Å and +0.23 Å, which corresponds to +12.8 km s^{-1} and +14.2 km s^{-1}. If the emission originated on the slowly rotating primary companion A ($V \sin i = 4$ km s^{-1}), it would be centered on the stellar line rather than shifted. We show below that on night 5 the lines of Ba and Bb were superimposed near their center-of-mass velocity, which should be displaced by +9.2 km s^{-1} relative to the RV of A according to the orbit (the masses of A and Ba+Bb being near-equal). The double peak on night 1 also matches the expected position of the emission from Ba and Bb. The non-detection of emission features on the other four nights could possibly be explained by variable activity of the M dwarfs.

4.4. Retrieval of the Ba and Bb Signature by Cross-correlation

We detect the signature of absorption lines belonging to Ba and Bb by correlating the residual spectra (after subtracting the template, see above) with the solar or Arcturus masks (the latter is analogous to the solar binary mask but uses the digital Arcturus spectrum from the same source). Only wavelengths shorter than 6500 Å are used in the correlation. The resulting CCF has a weak narrow feature centered on the RV of A (Figure 4). This feature originates because the resolution of the template spectrum is slightly less than the resolution of the nightly spectra owing to small residual alignment errors in the template creation. The sign and intensity of this feature depend on the relative degree of smoothing applied to the spectra and the template.

Apart from the central feature, we see additional dips with variable position and intensity, presumably produced by Ba and Bb. Gaussian approximations of the strongest dips have FWHM between 15 and 23 km s^{-1} and equivalent width of about

---

[2] NOAO data archive: ftp://ftp.noao.edu/catalogs/arcturusatlas.

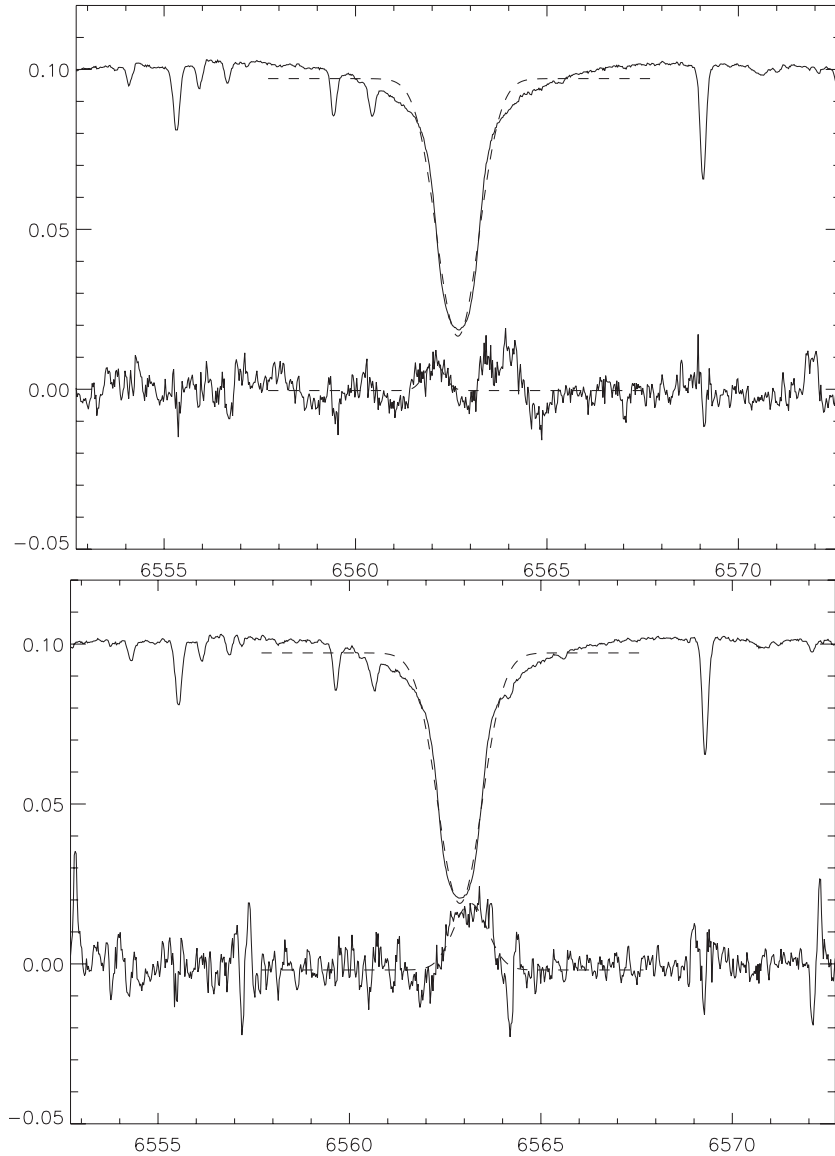**Figure 3.** Variable features in the Hα line on the night 1 (top panel) and on the night 5 (bottom panel). In each panel the upper curves show the continuum-normalized spectrum scaled by 0.1, with a Gaussian fit to the Hα (dashed line). The lower curves show the residuals after template subtraction.

0.0017 km s^{-1}. The star gives a CCF with equivalent width of 3.54 km s^{-1} for the Arcturus mask, so the dip ratio corresponds to the flux difference on the order of 5.8^m (we neglect here the different match of the Arcturus mask with the late-type spectrum of Ba on one hand and with the G0V spectrum of A on the other hand). A fake companion of 0.5% relative intensity (5.75^m fainter than the primary) is readily detectable by this method (see the upper curve in Figure 4).

The curves in Figure 4 give an impression of secondary lines moving with an amplitude of $\sim$80 km s^{-1}. We found a tentative circular orbit of Ba,Bb with a period of 3.666 d, semi-amplitude $K_1 = K_2 = 83$ km s^{-1}, γ-velocity +26 km s^{-1}, and initial epoch (RV maximum) JD 2456166.45. The data at hand are not sufficient for the orbit determination and the above elements are only a guess. The dashed and dotted lines in Figure 4 are Gaussian dips corresponding to the Ba and Bb components, respectively, and positioned according to this tentative orbit (not fitted to the CCF). The assumed amplitudes of both Gaussians are -0.0007, and their FWHM is 16 km s^{-1}. On night 1 we clearly see both dips. On nights 3 and 4 the CCFs of residuals look almost identical; the dips are near the maximum separation.

Remember that the template includes the average spectrum of Ba and Bb, so their lines near maximum separation (the most frequent situation) are partially subtracted, leaving only small residuals. On night 5 the dips overlap near the γ-velocity.

The reality of the detection of Ba and Bb was checked by correlating the residuals with the synthetic spectrum of a late-type dwarf. We used the $R = 500,000$ spectrum from Bertone et al. (2008)[3] with parameters $T_e = 4000$ K, $\log g = 5.0$, and solar metallicity. The resulting CCF should have a peak corresponding to the velocity of the secondary. Indeed, we see in Figure 5 positive features at approximately same velocities as the dips in Figure 4. To highlight these features, we again overplot fiducial Gaussians with an amplitude of +0.00007 and velocities predicted by the tentative Ba,Bb orbit.

The case for the component B being a binary is very strong. Its high mass, position in the CMD, variable emission, and moving absorption lines all confirm this hypothesis. The RV semi-amplitude in a spectroscopic binary with a circular edge-on orbit of period P days is $A_0 = 213 P^{-1/3} M_2 (M_1 + M_2)^{-2/3}$ km s^{-1},

---

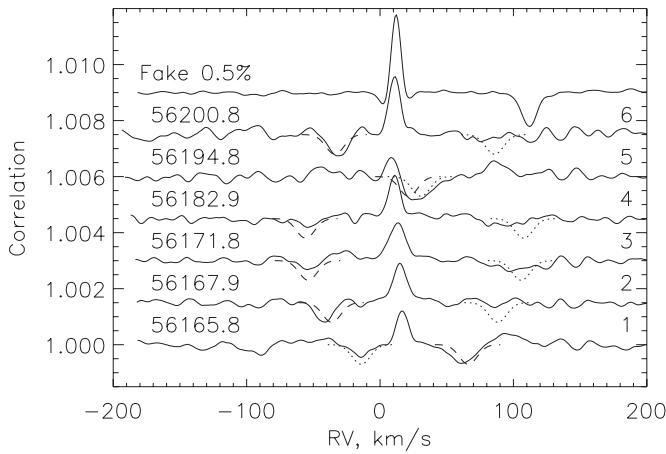[3] http://www.inaoep.mx/˜modelos/bluered/documentation.html

Figure 4. Correlation functions of residuals with the Arcturus mask for 6 nights (from bottom up, displaced by 0.0015 per night). The horizontal axis corresponds to the heliocentric RV. The upper curve is correlation with the template to which a fake companion of 0.5% intensity and +100 km s^{-1} RV shift is added. The dashed and dotted lines show suggested positions of the dips corresponding to Ba and Bb components, respectively, moving on a 3.7 day orbit. Numbers on the left are Julian dates, numbers on the right are the nights.

Figure 5. Correlation functions of residuals with the M-star synthetic spectrum for six nights (from bottom up), same as Figure 4.

or 69 km s^{-1} for $P = 3.7$ days, assuming $M_1 = M_2 = 0.5\,M_\odot$. The RV amplitude of our tentative Ba,Bb orbit is therefore in qualitative agreement with its period.

5. DISCUSSION

The triple system κ For consists of the main slightly evolved (age 4–6 Gyr) component A of 1.2 $M_\odot$, and a pair of M dwarfs of $\sim$0.5 $M_\odot$ each on a tight orbit with a tentative period of 3.7 d. The masses of A and Ba+Bb are nearly equal.

Further spectroscopic observations of κ For are needed to confirm the tentative period of Ba,Bb and to determine its orbit and mass. High-resolution spectroscopy in the near-infrared where the contrast of Ba,Bb is more favorable will help in this endeavor (e.g., Bender & Simon 2008). Given the short period, eclipses in Ba,Bb are likely, but their photometric detection presents a challenge because of the small (sub-percent) amplitude in the combined visible light. Precise photometry will eventually detect flares on the active M dwarfs. Long-term monitoring of both orbits will lead to the accurate measurement of the distance and the masses of all three stars.

Until now, the triple nature of κ For was not recognized despite its closeness to the Sun. The survey of Raghavan et al. (2010) lists it only as a binary. The question is how many more such systems are we missing? This relates to the ways of discovering sub-systems in the faint secondary companions.

The binarity of B was revealed by its unusually high mass. Overmassive companions can be detected by astrometry quite easily, comparing the photo-center axis α with the estimated full axis a (see Equation (1)), if the astrometric orbit and parallax are known. However, reliable astrometric orbits are rare. Acceleration measured by *Hipparcos* can also be used to estimate the mass ratio in binaries with reliably known visual or astrometric orbits. On the other hand, an excess of the total mass in orbital visual binaries with known parallax is a less promising way of finding such sub-systems because of the typically large uncertainties in both measured and modeled masses. Overmassive (binary) secondaries also can be detected by a high minimum mass inferred from a spectroscopic orbit, as, e.g., in the case of the quadruple system HD 27638 (Tokovinin & Gorynya 2001; Torres 2006). Overmassive but
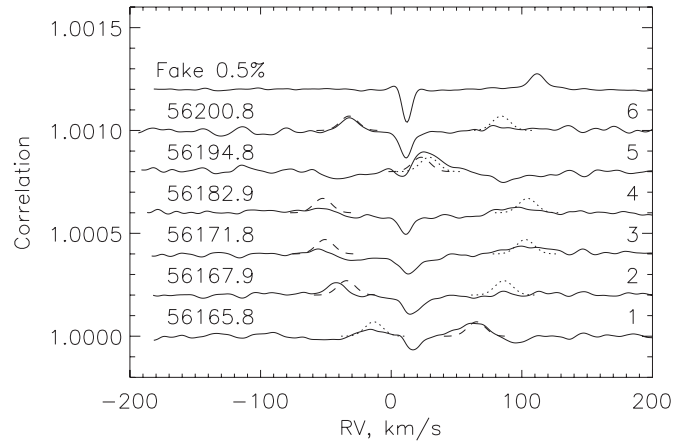
invisible companions could be white dwarfs; distinguishing them from tight pairs of red dwarfs usually requires some sort of photometry. When the resolved photometry of the secondary companion in two colors is available (e.g., from speckle interferometry), it can be placed on the CMD and detected as a binary by an excess in luminosity. Last but not least, spatial resolution of the sub-systems is the most direct and powerful method; if the period of Ba,Bb were longer than $\sim$0.5 yr (semimajor axis >30 mas), it would have been resolved at SOAR.

Statistical modeling done by Tokovinin et al. (2012) hints that 10%–20% of nearby solar-type astrometric binaries found by *Hipparcos* could have "massive" secondaries (sub-systems or white dwarfs). This conclusion, however, depends on several assumptions in the model. The detection techniques outlined above can be applied systematically to nearby binaries to better constrain the fraction of massive secondaries without making any assumptions. If sub-systems in the secondary companions are indeed as frequent as in the primaries, the known number of hierarchical triples will be nearly doubled, changing the multiplicity statistics dramatically.

Origins of multiple stars are still actively researched and debated, and different theories are tested by their predictions about multiplicity. For example, chaotic N-body dynamics rarely produces pairs of low-mass stars revolving around more massive primaries; rather, the primary itself is likely to end up in a close pair while the least massive body is ejected into a distant orbit around it (Delgado-Donate et al. 2003). Fragmentation of rotating cores makes the opposite prediction where the sub-systems in primary or secondary components are equally likely to form, being a natural sink of the angular momentum. In this paradigm, stars are often born as quadruples, but some inner sub-systems subsequently merge. Originally κ For could have consisted of two pairs of similar 0.5 $M_\odot$ stars. One pair had merged long time ago and became the present-day primary, while the other pair Ba,Bb is still here.

Binary secondary companions such as the one of κ For have implications for the search of exo-planets. If the period of Ba,Bb were few months or years, the weak secondary lines would always blend with the lines of A and create a small periodic RV signal that could be mistaken for an exo-planet signature, as, e.g., in HD 19994 (Röll et al. 2010).

Facilities: SOAR, CTIO:1.5m, Gemini-South

REFERENCES

Abt, H. A., & Willmarth, D. 2006, ApJS, 162, 207
Bender, C., & Simon, M. 2008, ApJ, 689, 416
Bertone, E., Buzzoni, A., Chavez, M., & Rodriguez-Merino, L. H. 2008, A&A, 485, 823
Campbell, W. W., & Moore, J. H. 1928, PLicO, 16, 1
Chun, M., Toomey, D., Wahhaj, Z., et al. 2008, Proc. SPIE, 7015, 70151V
Delgado-Donate, E. J., Clarke, C. J., & Bate, M. 2003, MNRAS, 342, 926
Endl, M., Kürster, M., Els, S., et al. 2002, A&A, 392, 671
ESA 1997, The *Hipparcos* and *Tycho* Catalogues (ESA SP-1200; Noordwijk: ESA)
Girardi, L., Bressan, A., Bertelli, G., & Chiosi, C. 2000, A&AS, 141, 371
Gontcharov, G. A., Andronova, A. A., & Titov, O. A. 2000, A&A, 355, 1164
Goncharov, G. A., & Kiyaeva, O. V. 2002, SvAL, 28, 261
Guedel, M., Schmitt, J. H. M. M., & Benz, A. O. 1995, A&A, 302, 775
Hartkopf, W. I., Tokovinin, A., & Mason, B. D. 2012, AJ, 143, 42
Hinkle, K., Wallace, L., Valenti, J., & Harmer, D. 2000, Visible and Near Infrared Atlas of the Arcturus Spectrum 3727–9300 Å (San Francisco, CA: ASP)
Lafrenière, D., Doyon, R., Marois, C., et al. 2007, ApJ, 670, 1367
Makarov, V. V., & Kaplan, G. H. 2005, AJ, 129, 2420
Mason, B. D., Wycoff, G. L., Hartkopf, W. I., Douglass, G. G., & Worley, C. E. 2001, AJ, 122, 3466
Nakajima, T., & Morino, J.-I. 2012, AJ, 143, 2
Nidever, D. L., Marcy, G. W., Butler, R. P., Fischer, D. A., & Vogt, S. S. 2002, ApJS, 141, 503
Nielsen, E. L., & Close, L. M. 2012, ApJ, 717, 878
Nordström, B., Mayor, M., Andersen, J., et al. 2004, A&A, 418, 989
Raghavan, D., McAlister, H. A., Henry, T. J., et al. 2010, ApJS, 190, 1
Röll, T., Seifahrt, A., Neuhuser, R., & Köhler, R. 2010, in ASP Conf. Ser. 435, Binaries—Key to Comprehension of the Universe, ed. A. Prsa & M. Zejda (San Francisco, CA: ASP), 419
Schwab, Ch., Spronck, J., Tokovinin, A., et al. 2012, Proc. SPIE, 8446, 84460B
Soubiran, C., Le Campion, J.-F., Cayrel de Strobel, G., & Caillo, A. 2010, A&A, 515, A111
Tokovinin, A., & Cantarutti, R. 2008, PASP, 120, 170
Tokovinin, A., Hartung, M., Hayward, Th. L., & Makarov, V. V. 2012, AJ, 144, 7
Tokovinin, A., Mason, B. D., & Hartkopf, W. I. 2010, AJ, 139, 743
Tokovinin, A. A., & Gorynya, N. A. 2001, A&A, 374, 227
Torres, G. 2006, AJ, 131, 1702
Trilling, D. E., Bryden, G., Beichman, C. A., et al. 2008, ApJ, 674, 1086
van Leeuwen, F. 2007, A&A, 474, 653